Topological invariants for interacting systems: From twisted boundary conditions to center-of-mass momentum

Ling Lin,[1,2,3] Yongguan Ke,[2,3,*] and Chaohong Lee[1,2,3,†]

[1]*College of Physics and Optoelectronic Engineering, Shenzhen University, Shenzhen 518060, China*

[2]*Guangdong Provincial Key Laboratory of Quantum Metrology and Sensing and School of Physics and Astronomy, Sun Yat-Sen University (Zhuhai Campus), Zhuhai 519082, China*

[3]*State Key Laboratory of Optoelectronic Materials and Technologies, Sun Yat-Sen University (Guangzhou Campus), Guangzhou 510275, China*

(Received 14 November 2022; revised 15 March 2023; accepted 21 March 2023; published 30 March 2023)

Beyond the well-known topological band theory for single-particle systems, it is a great challenge to characterize the topological nature of interacting multiparticle quantum systems. Here, we uncover the relation between topological invariants defined through the twisted boundary condition (TBC) and the center-of-mass (c.m.) momentum state in multiparticle systems. We find that the Berry phase defined through the TBC can be equivalently obtained from the multiparticle Wilson loop formulated by c.m. momentum states. As the Chern number can be written as the winding of the Berry phase, we consequently prove the equivalence of Chern numbers obtained via TBC and c.m. momentum state approaches. As a proof-of-principle example, we study topological properties of the Aubry-André-Harper model. Our numerical results show that the TBC approach and c.m. approach are well consistent with each other for both the many-body case and the few-body case. Our work lays a concrete foundation and provides insights for exploring multiparticle topological states.

DOI: 10.1103/PhysRevB.107.125161

I. INTRODUCTION

Since the discovery of the quantum Hall effect [1], topological quantum states have been widely and intensively studied. Owing to topological band theory, various quantum topological states have been successfully found in noninteracting systems [2–5]. However, in the presence of particle-particle interaction, because the single-particle quasimomentum is not a good quantum number, topological band theory usually fails. In interacting many-body quantum systems, different theoretical frameworks are developed to explore fascinating strongly correlated topological phases such as the fractional quantum Hall effect [6–8].

The first attempt is to introduce the twisted boundary condition (TBC) to define a topological invariant [9–18] for interacting many-body quantum systems. Similar to the periodic boundary condition (PBC), under the TBC, the boundaries along the same direction are glued together. The essential difference is that particles gain extra phases when they go through the boundaries under the TBC. The extra phase, which is known as the twist angle, can be considered a result of inserting magnetic flux [19,20] whose change will induce the flow of current [21,22]. Topological invariants defined via the twist angle have successfully explained topological features related to the system's response to external fields, such as the polarization (Berry phase) [23–26] and the quantized Hall conductance [27].

In recent years, a new approach has been proposed via the co-translation symmetry [28–30], with which the total energy remains unchanged when all particles as a whole are shifted by unit cells. The co-translation symmetry supports the c.m. quasimomentum as a good quantum number, and enables few-body topological band theory, in which topological invariants of gapped few-body Bloch bands can be defined via c.m. quasimomentum states [28–30]. Here, "few-body" means that the total particle number is fixed as a finite value N (even in the thermodynamic limit $L \to \infty$). With this approach, exotic interacting topological phases have been uncovered, such as topological bound edge states [28,29,31], topologically resonant tunnelings [30], and interaction-induced Thouless pumping [31].

While extensive interests have appeared in few-body topological states [28–39], it is more challenging and appealing to study topological states in many-body systems, where the filling factor $\nu = N/L$ keeps a finite value (even in the thermodynamic limit $L \to \infty$). In fact, the number of gapped many-body ground states strongly depends on the filling factor [40]. In contrast to the continuous band structure in few-body systems, a many-body gapped ground-state manifold may only consist of finite degenerate eigenstates with certain quasimomenta, as depicted in Fig. 1(a). It seems that there is no well-defined band structure for many-body systems. To date, how to utilize quasimomentum states to characterize many-body topological states remains vague.

Although the TBC approach and the center-of-mass (c.m.) momentum approach seem apparently different, they can independently and faithfully define topological invariants for interacting multiparticle systems. To date, there has been no

*keyg@mail2.sysu.edu.cn

†chleecn@szu.edu.cn, chleecn@gmail.com

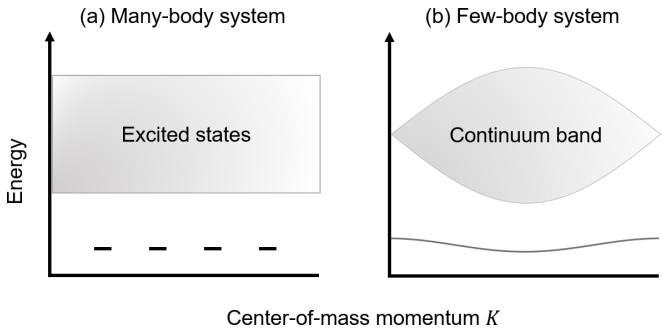

FIG. 1. Illustrative diagram for low-lying energy spectra of (a) many-body systems and (b) few-body systems under the PBC. For many-body systems, the degeneracy of the gapped ground-state manifold is finite, which strongly depends on the filling factor $\nu = N/L$. Here, we show the fourfold-degenerate ground states as an example. For few-body systems, there appears bandlike structure. Bands are dispersive and continuous in the thermodynamic limit. When the interaction is strong enough, there appears a gapped isolated band emerging from the continuum band, which usually corresponds to bound states.

comparison of the physics obtained from applying the two approaches to the same system. Understanding the relation between the two approaches can give insights into the foundation of interacting topological states. It is already known that threading a magnetic field to a system will induce a shift of the c.m. quasimomentum, indicating that the twisted angle has the same status of the c.m. quasimomentum. However, it is unclear whether the topological invariants defined with these two approaches are equivalent.

In this work, we generalize the c.m. momentum approach to many-body systems by introducing the *multiparticle Wilson loop*, and systematically clarify the relation between the TBC approach and the c.m. momentum approach, as depicted in Fig. 2. Under the TBC, we classify two different gauges as (i) a boundary gauge in which the twist angle is only gained at the crossing boundary, and (ii) a periodic gauge in which the twist angle is uniformly distributed at each hopping term. With the periodic gauge under the TBC, the co-translation symmetry is restored, and the c.m. momentum is related to the twist angle. The Berry phases defined via the twist angle under boundary and periodic gauges only differ by a trivial classical polarization, dubbed the TBC Berry phase for brevity. Under the PBC, by introducing the multiparticle Wilson loop, the Berry phase can be obtained from the c.m. momentum states, dubbed the c.m. Berry phase for brevity. The multiparticle Wilson loop is a generalization from the single-particle Wilson loop, applicable to both few-body and many-body systems. By employing perturbative analysis, we uncover that the TBC Berry phase in periodic gauge can be equivalently obtained via c.m. quasimomentum states and is related to the c.m. Berry phase. Since the Chern number can be expressed as the winding of Berry phases in two-dimensional (2D) systems, the Chern numbers obtained via the TBC approach and the c.m. momentum approach are therefore equivalent. To verify our general arguments, we consider a Aubry-André-Harper (AAH) model and numerically compute the topological properties of the gapped state. Our results clearly show that the two Berry phases as well as the Chern numbers defined through the twist angle and the c.m. momentum state are consistent with each other in both the few-body and many-body cases.

The rest of this article is organized as follows. In Sec. II, we introduce and review some key properties of the twisted boundary condition and the co-translation symmetry. We then discuss the relation between the twist angle and the center-of-mass momentum. In Sec. III, we discuss the Berry phase and the Chern number defined through the twist angle and the c.m. momentum state. We derive the relation between the TBC Berry phase and the c.m. Berry phase by using

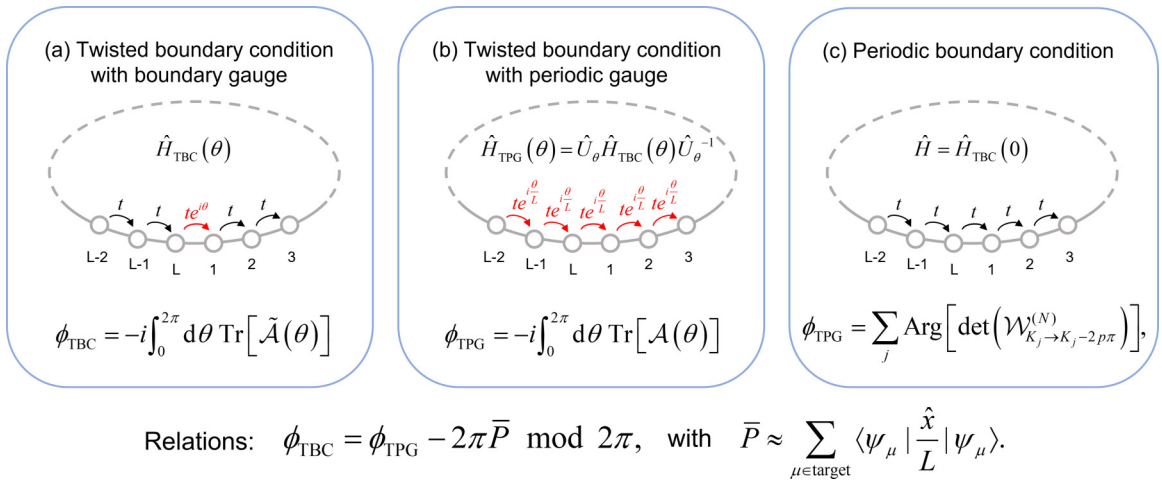

FIG. 2. Schematic demonstration of the simple tight-binding one-dimensional (1D) lattice under different boundary conditions and their corresponding Berry phases. (a) The general TBC with boundary gauge, (b) the TBC with periodic gauge, and (c) the periodic boundary condition. Under the boundary gauge (a), a particle only gains the phase when it crosses the boundary. Under the periodic gauge (b), a particle gains a "diluted" and homogeneous phase everywhere during the tunneling. The arrows indicate the tunneling of particles. Here t is the tunneling strength, θ is the twist angle, and L is the total number of cells. In both (b) and (c), the system possesses co-translational symmetry. The Berry phases corresponding to these three configurations as well as their relations are given below the diagrams. The central result is that the TBC Berry phase can be formulated by the c.m. momentum states.

perturbative expansion, and we discuss it respectively for many-body and few-body systems. In Sec. IV, we illustrate our general framework through the AAH model numerically and verify our arguments. In Sec. V, we briefly summarize and discuss our results.

II. TWISTED BOUNDARY CONDITION AND CENTER-OF-MASS MOMENTUM

In this section, we focus on discussing the relation between the twist angle under the TBC and the c.m. momentum state under the PBC. We will review the concepts of the twisted boundary condition, introduce the co-translation symmetry and the c.m. momentum, and then show the relation between the twist angle and the c.m. momentum state for both few-body and many-body systems.

A. Twisted boundary condition

To illustrate the TBC, we consider a generic form of the one-dimensional (1D) Hubbard-like Hamiltonian with two-body interaction,

$$\begin{aligned}\hat{H}_{\mathrm{TBC}}(\theta) &= -\sum_{x,d}\left(t_d e^{i\Theta_{x+d,x}}\hat{c}^{\dagger}_{x+d}\hat{c}_x + \mathrm{H.c.}\right)\\ &\quad + \sum_{x,d} V_d \hat{n}_{x+d}\hat{n}_x,\\ \Theta_{x+d,x} &= \begin{cases}\theta, & \langle x+d, x\rangle \text{ cross the boundary}\\ 0 & \text{otherwise,}\end{cases}\end{aligned} \tag{1}$$

in which $\hat{c}^{\dagger}_x$ ($\hat{c}_x$) is the creation (annihilation) operator at the xth site, and t_d and V_d are the tunneling strength and the two-body interaction strength, respectively. Tunneling and interaction are both finite range and only dependent on the relative distance d, which ensures the co-translation symmetry when $\theta = 0$. For simplicity, the lattice constant (i.e., the distance between two neighboring lattice sites) is set as $a = 1$. Meanwhile, the boundary is positioned between the Lth and first cells, and particles will gain phase only when tunneling through this boundary. Hence, the TBC can be viewed as a generalized periodic boundary condition [see Fig. 2(a) for a schematic demonstration]. It can be noted that Hamiltonian (1) is a periodic function of θ with the period 2π, that is,

$$\hat{H}_{\mathrm{TBC}}(\theta + 2\pi) = \hat{H}_{\mathrm{TBC}}(\theta). \tag{2}$$

The twist angle θ can be seen as a consequence of the insertion of a magnetic field, and particles feel gauge field in the lattice. Due to the gauge freedom, there are numerous conventions to determine how the vector potential (gauge field) distributes. Here, we choose a particular gauge by introducing the twist operator [41],

$$\hat{U}_\theta = \exp\left(i\frac{\theta}{L}\hat{x}\right), \tag{3}$$

in which $\hat{x} = \sum_x x\hat{n}_x$ is the position operator and L is length of the system. It can be checked that $\hat{U}_\theta \hat{c}^{\dagger}_x \hat{U}^{-1}_\theta = e^{i\frac{\theta}{L}x}\hat{c}^{\dagger}_x$. Under this twist transformation, the interaction type considered here remains unchanged. Then, the unitarily equivalent Hamiltonian reads as

$$\begin{aligned}\hat{H}_{\mathrm{TPG}}(\theta) &= \hat{U}_\theta \hat{H}_{\mathrm{TBC}}(\theta)\hat{U}^{-1}_\theta\\ &= -\sum_{x,d}\left(t_d e^{i\frac{\theta}{L}d}\hat{c}^{\dagger}_{x+d}\hat{c}_x + \mathrm{H.c.}\right)\\ &\quad + \sum_{x,d} V_d \hat{n}_{x+d}\hat{n}_x.\end{aligned} \tag{4}$$

The above transformation is generally called the large gauge transformation [42]. This particular unitary transformation means that we have chosen a gauge such that the vector field distributes uniformly, which is beneficial for us to establish the relation between the c.m. momentum and the twist angle later.

For convenience, we refer to the gauge choice in the transformed Hamiltonian (4) as the *periodic gauge* [see Fig. 2(b)], since the system satisfies the PBC. Notably, the periodicity of the Hamiltonian with respect to the twist angle θ is no longer 2π under this gauge. For the twist angle appearing only at the boundary [see Hamiltonian (1)], we call it the *boundary gauge* [see Fig. 2(a)]. In Fig. 2, we give a simple demonstration to show the essential differences among the TBC with the boundary gauge, the TBC with the periodic gauge, and the PBC without the twist angle. We would like to stress that the energy spectrum under the TBC is independent of the gauge choice.

B. Co-translation symmetry and center-of-mass momentum

In a general interacting multiparticle system, the single-particle translation symmetry is broken. However, the periodic system remains invariant after the translation of all particles when the interparticle interaction depends only on their relative distance. The translation of all N particles in a 1D lattice [28] can be expressed as

$$\hat{T}|x_1, x_2, \ldots, x_N\rangle = |x_1 + 1, x_2 + 1, \ldots, x_N + 1\rangle, \tag{5}$$

where $\hat{T}$ is the co-translation operator translating *all* particles for a unit cell, and $|x_1, x_2, \ldots, x_N\rangle$ is the multiparticle basis in position space, with x_j referring to the position of the jth particle. In our analysis, we assume the particles to be bosonic. For fermions, although the translation is similar, one should take care of the periodic boundary condition and the anticommutation relation (see Appendix A for detailed discussions).

Alternatively, we can use a c.m. position basis to expand the N-particle states,

$$|R, \beta\rangle \Leftrightarrow |x_1, x_2, \ldots, x_N\rangle, \tag{6}$$

where $R = \sum_j x_j/N$ is the c.m. position of the N particles, and β is an *abstract label* corresponding to the relative distribution of the N particles. Mathematically, β is uniquely determined by the set of all relative positions: $\{x_{i,j}\}_\beta$, $x_{i,j} = x_i - x_j$, $1 \leqslant i < j \leqslant N$. That is, $\{x_{i,j}\}_\beta$ contains the information of all relative positions between any pairs of particles. States labeled with the same β share the same relative distribution and can be translated to each other via the co-translation operation. In other words, these states form an invariant subspace for the representation of co-translation operator. The value of β depends on the geometry of the lattice and the total

number of particles, which grows rapidly with the system size and the total number of particles.

Since the co-translation operation will not change the relative positions between particles, we have

$$\hat{T}|R,\beta\rangle = |R+1,\beta\rangle. \tag{7}$$

The co-translation symmetry is defined by the commutation between the co-translation operator and the Hamiltonian: $[\hat{H},\hat{T}]=0$. If a multiparticle system under the PBC has co-translation symmetry, although the co-translation symmetry is broken under the TBC with boundary gauge, it can be restored under the TBC with periodic gauge.

Eigenstates of the co-translation operator can be expressed as

$$|K,\beta\rangle = \frac{1}{\sqrt{C_\beta}}\sum_R e^{iKR}|R,\beta\rangle, \tag{8}$$

where K is a good quantum number and C_β is the normalization factor. The summation in Eq. (8) is over all multiparticle position bases having the same relative distribution characterized by β, and the normalization factor depends on the number of these position bases. Here, similar to the single-particle quasimomentum, we can identify K as the c.m. quasimomentum, which is referred to as the c.m. momentum for brevity. Although K corresponds to the total momentum of all particles, we will use the terminology "c.m. momentum" to stress that it is the reciprocal lattice vector with respect to the center-of-mass position. It is easy to verify that Eq. (8) obeys

$$\begin{aligned}\hat{T}|K,\beta\rangle &= \frac{1}{\sqrt{C_\beta}}\sum_R e^{iK\cdot R}\hat{T}|R,\beta\rangle\\ &= \frac{1}{\sqrt{C_\beta}}\sum_R e^{iKR}|R+1,\beta\rangle\\ &= e^{-iK}\frac{1}{\sqrt{C_\beta}}\sum_R e^{iKR}|R,\beta\rangle\\ &= e^{-iK}|K,\beta\rangle.\end{aligned} \tag{9}$$

Consequently, the Hamiltonian can be block-diagonalized into the direct sum of c.m. Bloch Hamiltonians $h(K)$,

$$\hat{H} = \sum_K\sum_{\beta',\beta}|K,\beta'\rangle[h(K)]_{\beta',\beta}\langle K,\beta| = \bigoplus_K h(K), \tag{10}$$

where $[h(K)]_{\beta',\beta} = \langle K,\beta'|\hat{H}|K,\beta\rangle$. Thus, the eigenstate can be expressed as the linear combination of c.m. momentum basis $|K,\beta\rangle$,

$$\left|\psi_K^n\right\rangle = \sum_\beta u^n_{K,\beta}|K,\beta\rangle, \tag{11}$$

in which $u^n_{K,\beta}$ is the eigenvector of $h(K)$ satisfying $h(K)|u^n_K\rangle = E^n_K|u^n_K\rangle$, and n is the eigenenergy index of $h(K)$. We will call $|u^n_K\rangle$ the *c.m. momentum state*.

Under the PBC, applying the co-translation operator for L times will yield the same state: $\hat{T}^L|\psi\rangle = |\psi\rangle$. Hence, from Eq. (9), there is $K = 2\pi m/L$, $m\in\mathbb{Z}$. However, for a many-body system of indistinguishable particles, some specific distributions may reduce the needed times of co-translation symmetry to yield the same state. For example, let us consider two specific states in a simple one-dimensional lattice: (i) the state of all particles distributed uniformly, $|\ldots,1,1,1,\ldots\rangle$, and (ii) the state of the particles distributed uniformly only at odd or even sites, $|\ldots,0,2,0,2,\ldots\rangle$. Any co-translation operation will not change this state: $\hat{T}|\ldots,1,1,1,\ldots\rangle = |\ldots,1,1,1,\ldots\rangle$. According to Eq. (8), $|\ldots,1,1,1,\ldots\rangle$ can only be used to construct the c.m. momentum basis with $K=0$. For the state $|\ldots,0,2,0,2,\ldots\rangle$, applying the co-translation operator twice will bring the state back to the original state, and therefore it can only be used to construct the c.m. momentum basis with $K=0$ or $K=\pi$. This fact means that for different c.m. momenta, the number of the eigenstates of the co-translation operator can be different and therefore the matrix dimensions of the Bloch Hamiltonian $h(K)$ may be different. In dealing with the summation of different relative distributions in Eq. (10), we should carefully distinguish which states should be involved for a certain c.m. momentum.

In addition, the definition of position is essential in constructing the c.m. momentum basis. The c.m. position can be expressed as $R = R_i + R_\beta$ with an integer part $R_i\in\mathbb{Z}$ and a decimal part $R_\beta\in[0,1)$. Thus, according to Eq. (8), we have

$$|K+2\pi,\beta\rangle = e^{i2\pi R_\beta}|K,\beta\rangle. \tag{12}$$

In multiparticle systems, R_β is generally nonvanishing. The c.m. Bloch Hamiltonian then satisfies

$$[h(K+2\pi)]_{\beta',\beta} = [h(K)]_{\beta',\beta}e^{i2\pi(R_\beta - R_{\beta'})}. \tag{13}$$

In matrix notation, there is $h(K+2\pi) = \mathcal{R}_{2\pi}h(K)\mathcal{R}^{-1}_{2\pi}$, where $[\mathcal{R}_{2\pi}]_{\beta',\beta} = \delta_{\beta',\beta}e^{-i2\pi R_\beta}$. Hence, the c.m. momentum state satisfies $u^n_{K+2\pi,\beta} = e^{-i2\pi R_\beta}u^n_{K,\beta}$, and we have

$$\left|u^n_{K+2\pi}\right\rangle = \mathcal{R}_{2\pi}\left|u^n_K\right\rangle. \tag{14}$$

Such a kind of relation is very similar to the discussion for the TBC in Sec. II A. On the other hand, it can be checked that the eigenstate always satisfies the periodic condition

$$\begin{aligned}\left|\psi^n_{K+2\pi}\right\rangle &= \sum_\beta u^n_{K+2\pi,\beta}|K+2\pi,\beta\rangle\\ &= \sum_\beta u^n_{K,\beta}|K,\beta\rangle\\ &= \left|\psi^n_K\right\rangle.\end{aligned} \tag{15}$$

The above discussion for c.m. momentum states is very similar to the band theory for single-particle systems, and can also be generalized to higher-dimensional systems.

C. Connection between the twist angle and the center-of-mass momentum states

Below we show how the twist angle connects with the c.m. momentum states. First, we would like to discuss the general characteristics for both many-body and few-body systems. It can be noted that the co-translation symmetry is broken under the TBC with boundary gauge, i.e., $[\hat{H}_{\rm TBC}(\theta),\hat{T}]\neq 0$. Nevertheless, when the periodic gauge is imposed on the TBC, the system satisfies the PBC, and the co-translation symmetry is restored, i.e., $[\hat{H}_{\rm TPG}(\theta),\hat{T}]=0$. As discussed in Sec. II B, we can block-diagonalize the Hamiltonian in this situation and obtain the Bloch Hamiltonian $h(K,\theta)$ from the

c.m. momentum approach discussed above. Using Eq. (4), we can find that the matrix elements of the Bloch Hamiltonian satisfy the following relation:

$$\begin{aligned}
&[h(K,\theta+2\pi)]_{\beta',\beta}\\
&=\langle K,\beta'|\hat{H}_{\mathrm{TPG}}(\theta+2\pi)|K,\beta\rangle\\
&=\langle K,\beta'|\hat{U}_{2\pi}\hat{U}_{\theta}\hat{H}_{\mathrm{TBC}}(\theta)\hat{U}_{\theta}^{-1}\hat{U}_{2\pi}^{-1}|K,\beta\rangle\\
&=\langle K-N\delta K,\beta'|\hat{U}_{\theta}\hat{H}_{\mathrm{TBC}}(\theta)\hat{U}_{\theta}^{-1}|K-N\delta K,\beta\rangle\\
&=\langle K-N\delta K,\beta'|\hat{H}_{\mathrm{TPG}}(\theta)|K-N\delta K,\beta\rangle\\
&=[h(K-N\delta K,\theta)]_{\beta',\beta}, \qquad (16)
\end{aligned}$$

where $\delta K=2\pi/L$ is the minimum increment of the c.m. momentum, and we have used the relation

$$\begin{aligned}
\hat{U}_{2\pi}^{-1}|K,\beta\rangle&=\frac{1}{\sqrt{C_\beta}}\sum_R e^{iKR}e^{-i\frac{2\pi}{L}\hat{x}}|R,\beta\rangle\\
&=\frac{1}{\sqrt{C_\beta}}\sum_R e^{iKR}e^{-i\frac{2\pi}{L}NR}|R,\beta\rangle\\
&=\frac{1}{\sqrt{C_\beta}}\sum_R e^{i(K-N\delta K)R}|R,\beta\rangle\\
&=|K-N\delta K,\beta\rangle. \qquad (17)
\end{aligned}$$

Here $\hat{U}_{2\pi}$ is also called the twist operator [43] and it satisfies $\hat{T}(\hat{U}_{2\pi}^{-1}|K,\beta\rangle)=e^{i(K-N\delta K)}(\hat{U}_{2\pi}^{-1}|K,\beta\rangle)$.

From Eq. (16), we find that the Bloch Hamiltonian $h(K)$ satisfies the important relation

$$h(K,\theta+2\pi)=h(K-N\delta K,\theta), \qquad (18)$$

and the corresponding c.m. momentum state [the eigenstate of $h(K,\theta)$] will satisfy the following relation:

$$\left|u_K^n(\theta+2\pi)\right\rangle=\left|u_{K-N\delta K}^n(\theta)\right\rangle. \qquad (19)$$

This means that the twist angle continuously connects c.m. momentum states in different sectors under the periodic gauge. Moreover, eigenstates of the Hamiltonian under the TBC with periodic gauge (4) satisfy a rather different relation:

$$\begin{aligned}
&\left|\psi_{K+N\delta K}^n(\theta+2\pi)\right\rangle\\
&=\sum_\beta u_{K+N\delta K,\beta}^n(\theta+2\pi)|K+N\delta K,\beta\rangle\\
&=\sum_\beta u_{K,\beta}^n(\theta)|K+N\delta K,\beta\rangle\\
&=\sum_\beta u_{K,\beta}^n(\theta)\hat{U}_{2\pi}|K,\beta\rangle\\
&=\hat{U}_{2\pi}\left|\psi_K^n(\theta)\right\rangle. \qquad (20)
\end{aligned}$$

By multiplying $\hat{U}_{\theta+2\pi}^{-1}$ on both sides of Eq. (20), one can transform the periodic gauge back to the boundary gauge,

$$\left|\tilde{\psi}_{K+N\delta K}^n(\theta+2\pi)\right\rangle=\left|\tilde{\psi}_K^n(\theta)\right\rangle, \qquad (21)$$

where $|\tilde{\psi}_K^n(\theta)\rangle$ are the eigenstates of the TBC Hamiltonian under boundary gauge $\hat{H}_{\mathrm{TBC}}(\theta)$. Note that the co-translation symmetry is broken under the boundary gauge, and the c.m. momentum K is not a good quantum number for $\hat{H}_{\mathrm{TBC}}(\theta)$. However, there is still a one-to-one correspondence between the eigenstates of the periodic-gauge Hamiltonian and the boundary-gauge Hamiltonian since they are related by the unitary transformation: $|\psi_\mu(\theta)\rangle=\hat{U}_\theta|\tilde{\psi}_\mu(\theta)\rangle$. Here, μ denotes the index of eigenstates. Thus, we can still assign the quantum numbers $\{K,n\}$ to the eigenstates of $\hat{H}_{\mathrm{TBC}}(\theta)$ such that

$$|\tilde{\psi}_\mu(\theta)\rangle\equiv\left|\tilde{\psi}_K^n(\theta)\right\rangle. \qquad (22)$$

Under the boundary gauge, a notable consequence of Eq. (21) is that when the twist angle θ flows from 0 to 2π, each of the eigenstates will flow *adiabatically* to another eigenstate if N/L is not an integer, although the TBC Hamiltonian under the boundary gauge flows back to the same Hamiltonian.

According to Eq. (18), the eigenenergy will also follow the relation

$$E_K^n(\theta+2\pi)=E_{K-N\delta K}^n(\theta). \qquad (23)$$

From Eq. (23), we can see that the eigenenergies change continuously from $E_K^n(0)$ to $E_{K-N\delta K}^n(0)$ when the twist angle θ changes adiabatically 2π. It has been proven that the finite excitation gap is not affected by the twist angle θ in the thermodynamic limit [41]. Physically, it can be understood that the change of the twist angle at the boundary will not affect the bulk when the system is away from the critical point. This means that if $E_K^n(0)$ is the eigenenergy of the gapped ground state, then the eigenstate whose eigenenergy is $E_{K-N\delta K}^n(0)$ also belongs to the ground-state manifold. Thus, the degeneracy of the gapped ground-state manifold depends on the filling factor $\nu=N/L$. For example, consider the case of a filling factor $\nu=N/L=p/q$ with p and q being co-prime numbers. The degeneracy of the ground states must be the multiple of q.

The above discussion on the relation between the twist angle and the c.m. momentum is general, and the results can be applied to both many-body and few-body systems. Actually, this result is in agreement with the celebrated Lieb-Shultz-Mattis (LSM) theorem [40,43–47].

III. BERRY PHASE AND CHERN NUMBER

In this section, we study the Berry phases and the Chern numbers defined with the TBC and the c.m. momentum states, respectively. In noninteracting lattice systems, it is known that the Berry phase defined through the single-particle quasimomentum is related to polarization [24–26,48]. By choosing an appropriate gauge for the Berry connection (Berry vector potential), the Chern number for 2D systems can be expressed as the winding of the Berry phase. The adiabatic change of Berry phase reflects the flow of the current induced by modulation. The periodic modulation may result in a nontrivial Chern number, corresponding to the number of particles being pumped. Periodic modulations can be a time-dependent lattice potential applied to a 1D system, or a magnetic flux inserted in the 2D system in a cylinder geometry. The many-body Berry phase has been studied extensively [49]. In particular, when the system has some symmetries, the Berry phase is used as an order parameter to characterize the symmetry-protected topological phase [50,51]. Therefore, it is essential to investigate the Berry phase for interacting multiparticle systems.

A. Twisted boundary condition approach to Berry phase

In this section, we will present the Berry phase defined through the twist angle under two different gauges: the boundary gauge and the periodic gauge. We also discuss the gauge-invariant condition. Although the two cases are unitarily equivalent, their Berry phases differ by a classical polarization. Particularly, with the periodic gauge, one can expand the eigenstate up to the first order of θ/L, which allows us to relate the Berry phases respectively defined with the twist angle and the c.m. momentum later.

1. Boundary gauge

First, let us consider a 1D system under the TBC with the boundary gauge. Given a set of target states $\tilde{\mathcal{G}}(\theta)=\{|\tilde{\psi}_\mu(\theta)\rangle\}$ (which are gapped to other states), we write them as a vector $\tilde{\mathbf{\Psi}}_\theta=(|\tilde{\psi}_1(\theta)\rangle,\ldots,|\tilde{\psi}_{\mathcal{N}}(\theta)\rangle)$, in which $\mathcal{N}$ is the number of the target states. One can use the non-Abelian form to define the Berry phase with the twist angle,

$$\begin{aligned}\phi_{\mathrm{TBC}}&=-i\int_0^{2\pi}\mathrm{d}\theta\ \mathrm{Tr}[\tilde{\mathcal{A}}(\theta)],\\ \tilde{\mathcal{A}}(\theta)&=\tilde{\mathbf{\Psi}}_\theta^\dagger\partial_\theta\tilde{\mathbf{\Psi}}_\theta,\end{aligned}\tag{24}$$

where the minus sign is imposed for convenience.

Next, it is of importance to discuss when the Berry phase (24) is gauge invariant. Supposing a $U(\mathcal{N})$ gauge transformation, $\tilde{\mathbf{\Psi}}_\theta\to\tilde{\mathbf{\Psi}}'_\theta=\tilde{\mathbf{\Psi}}_\theta\tilde{\mathcal{U}}_\theta$ with $\tilde{\mathcal{U}}_\theta$ being a continuous function of θ, there is

$$\phi_{\mathrm{TBC}}\to\phi_{\mathrm{TBC}}-i\int_0^{2\pi}\mathrm{d}\theta\ \mathrm{Tr}(\tilde{\mathcal{U}}_\theta^\dagger\partial_\theta\tilde{\mathcal{U}}_\theta).\tag{25}$$

Note that the 2π periodicity of the Hamiltonian $\hat{H}_{\mathrm{TBC}}(\theta)$ does not mean its eigenstate will flow back to the original state when the twist angle varies 2π. According to Eq. (21), when the twist angle varies 2π, the boundary-gauge eigenstates will flow to a different eigenstate if N/L is not an integer. Therefore, the extra gauge term in Eq. (25) may not be zero. In other words, it seems that the TBC Berry phase (24) is gauge dependent. As discussed in the previous section, the twist angle will not change the spectral gap in the thermodynamic limit, and we have $\tilde{\mathcal{G}}(\theta+2\pi)=\tilde{\mathcal{G}}(\theta)$. This means that, under the gapped condition, any target state $|\tilde{\psi}_\mu(\theta)\rangle\in\tilde{\mathcal{G}}(\theta)$ will finally evolve into another eigenstate which still belongs to the same set of target states when the twist angle changes 2π, that is,

$$|\tilde{\psi}_\mu(\theta+2\pi)\rangle=|\tilde{\psi}_{\mu'}(\theta)\rangle\in\tilde{\mathcal{G}}(\theta).\tag{26}$$

Hence, we would like to impose $\tilde{\mathbf{\Psi}}_{\theta+2\pi}=\tilde{\mathbf{\Psi}}_\theta$ in practical calculations, and this leads to $\tilde{\mathcal{U}}_{\theta+2\pi}=\tilde{\mathcal{U}}_\theta$. Then, the extra term satisfies

$$\int_0^{2\pi}\mathrm{d}\theta\ \mathrm{Tr}(\tilde{\mathcal{U}}_\theta{}^\dagger\partial_\theta\tilde{\mathcal{U}}_\theta)=2m\pi,\quad m\in\mathbb{Z},\tag{27}$$

where we have used the fact that this integral produces the winding number of the unitary matrix $\tilde{\mathcal{U}}_\theta$. Therefore, we arrive at the conclusion that the TBC Berry phase modulo 2π is $U(\mathcal{N})$ gauge invariant as long as the target states are gapped.

2. Periodic gauge

On the other hand, one may wonder if we can define the Berry phase under the periodic gauge via the same form,

$$\begin{aligned}\phi_{\mathrm{TPG}}&=-i\int_0^{2\pi}d\theta\ \mathrm{Tr}[\mathcal{A}(\theta)],\\ \mathcal{A}(\theta)&=\mathbf{\Psi}_\theta^\dagger\partial_\theta\mathbf{\Psi}_\theta,\end{aligned}\tag{28}$$

where $\mathbf{\Psi}_\theta=(|\psi_1(\theta)\rangle,\ldots,|\psi_{\mathcal{N}}(\theta)\rangle)$ corresponds to a set of eigenstates under periodic gauge. In fact, the Berry phase in Eq. (28) is generally not gauge invariant, since the period of the Hamiltonian under periodic gauge, $\hat{H}_{\mathrm{TPG}}(\theta)$, is not 2π. Similarly, consider a $U(\mathcal{N})$ gauge transformation $\mathbf{\Psi}_\theta\to\mathbf{\Psi}'_\theta=\mathbf{\Psi}_\theta\mathcal{U}_\theta$ for a set of target states $\mathcal{G}(\theta)=\{|\psi_\mu(\theta)\rangle\}$ gapped to other states. This gauge transformation leads to

$$\phi_{\mathrm{TPG}}\to\phi_{\mathrm{TPG}}-i\int_0^{2\pi}d\theta\ \mathrm{Tr}(\mathcal{U}_\theta^\dagger\partial_\theta\mathcal{U}_\theta).\tag{29}$$

Apparently, the period of $\mathcal{U}_\theta$ is not 2π, which means the integral in Eq. (29) modulo 2π is not necessarily zero, implying that Eq. (28) is not gauge invariant. To make the Berry phase (28) gauge invariant, one can manually fix the gauge. As discussed in previous sections, the gapped target states satisfy $|\psi_\mu(\theta+2\pi)\rangle=\hat{U}_{2\pi}|\psi_{\mu'}(\theta)\rangle$, in which $|\psi_{\mu'}(\theta)\rangle\in\mathcal{G}(\theta)$. With this, we can also impose the following relation,

$$\mathbf{\Psi}_{\theta+2\pi}=\hat{U}_{2\pi}\mathbf{\Psi}_\theta,\tag{30}$$

and then the $U(\mathcal{N})$ gauge transformation will satisfy the periodic relation $\mathcal{U}_{\theta+2\pi}=\mathbf{\Psi}_{\theta+2\pi}^\dagger\hat{U}_{2\pi}\mathbf{\Psi}_\theta\mathcal{U}_\theta=\mathcal{U}_\theta$. Hence, similar to Eq. (27), the extra gauge term will only produce an integer multiple of 2π,

$$i\int_0^{2\pi}d\theta\ \mathrm{Tr}(\mathcal{U}_\theta^\dagger\partial_\theta\mathcal{U}_\theta)=2m\pi,\quad m\in\mathbb{Z},\tag{31}$$

and the Berry phase under periodic gauge [Eq. (28)] is gauge invariant modulo 2π now. This is particularly useful in practical computation.

3. Relation of the Berry phases for different gauges

By using the relation between the eigenstates under the two different gauges, $\mathbf{\Psi}_\theta=\hat{U}_\theta\tilde{\mathbf{\Psi}}_\theta$, the Berry phase (28) becomes

$$\begin{aligned}\phi_{\mathrm{TPG}}&=-i\int_0^{2\pi}\mathrm{d}\theta\ \mathrm{Tr}[\mathcal{A}(\theta)]\\ &=-i\int_0^{2\pi}\mathrm{d}\theta\ \mathrm{Tr}[\tilde{\mathcal{A}}(\theta)]\\ &\quad-i\int_0^{2\pi}\mathrm{d}\theta\ \mathrm{Tr}[\tilde{\mathbf{\Psi}}_\theta^\dagger\hat{U}_\theta^\dagger(\partial_\theta\hat{U}_\theta)\tilde{\mathbf{\Psi}}_\theta]\\ &=\phi_{\mathrm{TBC}}+2\pi\bar{P},\end{aligned}\tag{32}$$

where

$$\bar{P}=\frac{1}{2\pi L}\int_0^{2\pi}\mathrm{d}\theta\ \mathrm{Tr}(\tilde{\mathbf{\Psi}}_\theta^\dagger\hat{x}\tilde{\mathbf{\Psi}}_\theta)\tag{33}$$

corresponds to the classical polarization averaged over the twist angle. Formula (32) reveals that the two TBC Berry phases differ by a classical polarization, which is consistent

with the results of Ref. [14] where the target state only consists of one unique eigenstate.

On the other hand, it is known that the definition of the position is somewhat arbitrary due to the TBC. Equation (32) suggests that the TBC Berry phases under either the boundary gauge or the periodic gauge are affected by the choice of the position operator $\hat{x}$. Apparently, the TBC Berry phase under the boundary gauge [Eq. (24)] does not involve any position information except for the determination of boundary. It should be irrelevant to how the position operator is defined. Thus, we can conclude that only the TBC Berry phase under the periodic gauge (ϕ_{TPG}) depends on the definition of the position operator. This is similar to the single-particle situation, where the Berry phase can be split into the intercellular and intracellular parts [52]. Correspondingly, the intercellular Berry phase in the single-particle case corresponds to the TBC Berry phase (24), and the intracellular Berry phase corresponds to the classical polarization part. Unlike Ref. [52], the relation obtained here is purely based on the TBC, and can be applied to both single-particle and multiparticle systems without requiring translation symmetry.

4. Perturbative analysis for periodic gauge

To see the perturbative nature of the TBC Berry phase, let us consider a system described by the Hamiltonian under the TBC with periodic gauge, as introduced in Eq. (4). In this condition, the co-translation symmetry is preserved. We can label the eigenstate by good quantum numbers: $|\psi_\mu(\theta)\rangle \equiv |\psi_K^n\rangle$. Since the tunneling is assumed to be finite range, it can be seen from Hamiltonian (4) that the twist angle always appears as an extremely small quantity θ/L in the thermodynamic limit. Hence, provided the tunneling is finite range, the eigenstate can be expanded in terms of θ/L:

$$\left|\psi_K^n(\theta)\right\rangle = \left|\psi_K^n(0)\right\rangle + \frac{\theta}{L}\left|\partial_{\theta/L}\psi_K^n(\theta)\right\rangle_{\theta=0} + O\left(\frac{1}{L^2}\right). \quad (34)$$

By taking derivatives for both sides, we have

$$\begin{aligned}\partial_\theta\left|\psi_K^n(\theta)\right\rangle &= \frac{1}{L}\left|\partial_{\theta/L}\psi_K^n(\theta)\right\rangle_{\theta=0} + O\left(\frac{1}{L^2}\right),\\ &= \left|\partial_\theta\psi_K^n(\theta)\right\rangle_{\theta=0} + O\left(\frac{1}{L^2}\right). \end{aligned} \quad (35)$$

Therefore, up to the first order of $\frac{\theta}{L}$, we obtain

$$\left\langle\psi_{K'}^{n'}(\theta)\middle|\partial_\theta\psi_K^n(\theta)\right\rangle = \left\langle\psi_{K'}^{n'}(0)\middle|\partial_\theta\psi_K^n(\theta)\right\rangle_{\theta=0} + O\left(\frac{1}{L^2}\right). \quad (36)$$

This means that, up to the first order of $\frac{1}{L}$, the quantity $\langle\psi_{K'}^{n'}(\theta)|\partial_\theta\psi_K^n(\theta)\rangle$ is independent of the twist angle θ. Then, we can set $\theta = 2\pi$ in Eq. (34),

$$\left|\partial_\theta\psi_K^n(\theta)\right\rangle_{\theta=0} = \frac{1}{2\pi}\left[\left|\psi_K^n(2\pi)\right\rangle - \left|\psi_K^n(0)\right\rangle\right] + O\left(\frac{1}{L^2}\right), \quad (37)$$

and therefore

$$\begin{aligned}\left\langle\psi_{K'}^{n'}(\theta)\middle|\partial_\theta\psi_K^n(\theta)\right\rangle &= \frac{1}{2\pi}\left\langle\psi_{K'}^{n'}(0)\middle|\psi_K^n(2\pi)\right\rangle\\ &\quad - \frac{1}{2\pi}\delta_{n',n}\delta_{K',K} + O\left(\frac{1}{L^2}\right). \end{aligned} \quad (38)$$

Furthermore, according to Eq. (20), one can use $|\psi_K^n(2\pi)\rangle = \hat{U}_{2\pi}|\psi_{K-N\delta K}^n(0)\rangle$ and find

$$\begin{aligned}\left\langle\psi_{K'}^{n'}(\theta)\middle|\partial_\theta\psi_K^n(\theta)\right\rangle &= \frac{1}{2\pi}\left\langle\psi_{K'}^{n'}(0)\middle|\hat{U}_{2\pi}\middle|\psi_{K-N\delta K}^n(0)\right\rangle\\ &\quad - \frac{1}{2\pi}\delta_{n',n}\delta_{K',K} + O\left(\frac{1}{L^2}\right). \end{aligned} \quad (39)$$

Hence, we can approximate the Berry connection as

$$\mathcal{A}(\theta) \approx \mathcal{M} - I_{\mathcal{N}}, \quad (40)$$

where $I_{\mathcal{N}}$ is an $\mathcal{N}\times\mathcal{N}$ identity matrix and $\mathcal{M}$ is an $\mathcal{N}\times\mathcal{N}$ matrix with elements

$$\mathcal{M}_{(n',K'),(n,K)} = \left\langle\psi_{K'}^{n'}(0)\middle|\hat{U}_{2\pi}\middle|\psi_{K-N\delta K}^n(0)\right\rangle. \quad (41)$$

In the above, $\mathcal{N}$ is the number of target states and we have dropped the notation of the twist angle since $\theta = 0$. This means that the Berry connection $\mathcal{A}(\theta)$ in Eq. (28) is independent of the twist angle θ up to the first order of $\frac{1}{L}$. Similarly, up to the first order of $\frac{1}{L}$, we can approximate the classical polarization (33) as

$$\bar{P} \approx \sum_{n,K}\left\langle\psi_K^n\middle|\frac{\hat{x}}{L}\middle|\psi_K^n\right\rangle. \quad (42)$$

We also find that, in the thermodynamic limit, the matrix $\mathcal{M}$ is approximately a unitary matrix in the subspace spanned by target states (see the detailed discussion in Appendix B). Then, in the thermodynamic limit, the TBC Berry phase (28) can be written as [53]

$$\phi_{\mathrm{TPG}} = \mathrm{Im}[\mathrm{Tr}(\mathcal{M} - I_{\mathcal{N}})] \approx \mathrm{Arg}[\det(\mathcal{M})]. \quad (43)$$

A similar approximation has been used in Ref. [15].

The above formula (43) is related to the polarization formula proposed by Resta [13], which has been widely applied to investigate the polarization of various systems, from noninteracting [54–57] to interacting [58,59] systems. It can be found that

$$\mathcal{M} = \mathbf{\Psi}_0^\dagger\hat{U}_{2\pi}\mathbf{\Psi}_0\mathcal{S}, \quad (44)$$

where $\mathcal{S}$ is an orthogonal matrix that permutes the order of the eigenstates in $\mathbf{\Psi}_0$ depending on the flow of the target states. Since the orthogonal matrix satisfies $\det(\mathcal{S}) = \pm 1$, the Berry phases obtained from the TBC method and the Resta formula may at most have a π phase difference.

B. Center-of-mass momentum approach to Berry phase

Next, let us discuss the Berry phase defined through c.m. momentum states. In few-body systems, the filling number tends to zero, $\nu = N/L \to 0$, while the total particle number N is fixed. In analogy to the single-particle system, the band structure appears, as demonstrated in Fig. 1(b). Hence, in the same fashion, it is desirable to define the Berry phase through c.m. momentum states

$$\phi = i\int_0^{2\pi} \mathrm{d}K\ \mathrm{Tr}(A_K), \quad (45)$$

in which $[A_K]_{m,n} = \langle u_K^m|\partial_K u_K^n\rangle$. To guarantee the gauge invariance, we have to impose $|u_{2\pi}^n\rangle = \mathcal{R}_{2\pi}|u_0^n\rangle$ according to Eq. (14). Equation (45) reflects the geometric phase gained by

the few-body system after traveling through the Brillouin zone adiabatically. This reveals the topological property of the Brillouin manifold with respect to the c.m. momentum state. In particular, Eq. (45) has been successfully used to investigate the topological properties of few-body bound states [28–31].

However, Eq. (45) cannot be applied to the many-body system, as the number of gapped ground states is finite, and therefore we cannot use the integral formulation. To unify the c.m. approach for few-body and many-body systems, it is desirable to use the Wilson loop to calculate the Berry phase. Recall that in the single-particle case, the Wilson loop reads as $\mathcal{W}^{(1)}_{K\to K-2\pi} = F^{(1)}_K F^{(1)}_{K-\delta K}\cdots F^{(1)}_{K-2\pi+\delta K}$, in which $[F^{(1)}_K]_{n',n} = \langle u^{n'}_K | u^{n}_{K-\delta K}\rangle$ and the superscript denotes the particle number. For the N-particle system with the filling number $\nu = N/L = p/q$, we propose that the *N-particle Wilson loop* should be modified as

$$\mathcal{W}^{(N)}_{K\to K-2p\pi} = F^{(N)}_K F^{(N)}_{K-N\delta K}\cdots F^{(N)}_{K-2p\pi+N\delta K}, \tag{46}$$

in which $[F^{(N)}_K]_{n',n} = \langle u^{n'}_K | u^{n}_{K-N\delta K}\rangle$. We can consider the N-particle Wilson loop as a generalization of the single-particle Wilson loop. The increment of the quasimomentum is $N\delta K$ for the N-particle system, and the range of the Wilson loop depends on the filling factor $\nu = N/L = p/q$. The Brillouin zone is now expanded p times to complete the loop. The c.m. Berry phase is therefore defined as

$$\phi_{\text{c.m.}}(K) = \text{Arg}\big[\det\big(\mathcal{W}^{(N)}_{K\to K-2p\pi}\big)\big], \tag{47}$$

where K is the starting point of the Wilson loop. Note that one should impose the relation in Eq. (14) to guarantee the gauge invariance.

C. Connection between the TBC Berry phase and the center-of-mass Berry phase

From Eq. (41), one can find that the matrix $\mathcal{M}$ has a block-diagonal structure

$$\begin{aligned}
&\mathcal{M}_{(n',K'),(n,K)}\\
&= \big\langle \psi^{n'}_{K'}\big|\hat{U}_{2\pi}\big|\psi^{n}_{K-N\delta K}\big\rangle\\
&= \sum_{\beta',\beta}\big(u^{n'}_{K',\beta'}\big)^{*} u^{n}_{K,\beta}\langle K',\beta|\hat{U}_{2\pi}|K-N\delta K,\beta\rangle\\
&= \big\langle u^{n'}_K\big|u^{n}_{K-N\delta K}\big\rangle\delta_{K',K},
\end{aligned} \tag{48}$$

and we can write $\mathcal{M} = \bigoplus_K F^{(N)}_K$ with $[F^{(N)}_K]_{n',n} = \langle u^{n'}_K | u^{n}_{K-N\delta K}\rangle$ and the indices running over all c.m. momenta of the target states $K \in \{K_{\text{target}}\}$. For convenience, we use the superscript (N) in $F^{(N)}_K$ to emphasize that the increment of the c.m. momentum is $N\delta K$. Then, under the periodic gauge, the TBC Berry phase can be written as

$$\begin{aligned}
\phi_{\text{TPG}} &= \text{Arg}[\det(\mathcal{M})]\\
&= \sum_{K\in\{K_{\text{target}}\}}\text{Arg}\big[\det\big(F^{(N)}_K\big)\big].
\end{aligned} \tag{49}$$

As the matrix $\mathcal{M}$ is defined via the states for $\theta = 0$ (i.e., the states for the Hamiltonian under the PBC), the above formula implies that the TBC Berry phase can be equivalently formulated by the c.m. momentum states under the PBC.

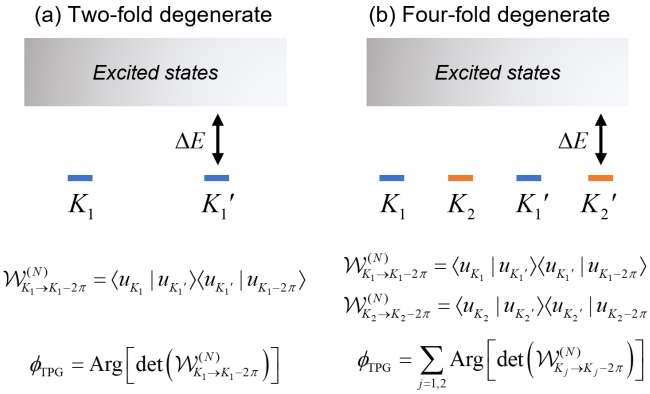

FIG. 3. Illustrative example for the TBC Berry phase and the multiparticle Wilson loop. [(a), (b)] Two different cases of the target states at $\nu = 1/2$ filling. The color distinguishes two different sets of the c.m. momentum states, as defined in Eq. (50). In each set, c.m. momenta only differ by an integer multiple of $N\delta K$. In (a), the target states only form one single multiparticle Wilson loop. In (b), the target states form two multiparticle Wilson loops.

As discussed in Sec. II C, the twist angle continuously connects certain c.m. momentum sectors. We can collect these c.m. momenta to form a subset

$$\{\tilde{K}_j\} = \left\{K\middle|K = K_j - 2n\pi\frac{p}{q},\ n = 0,1,\ldots,q-1\right\}, \tag{50}$$

where K_j is one of the c.m. momenta in the target states. Hence, the c.m. momenta in the target states can be written as the union of these subsets, $\{K_{\text{target}}\} = \cup_j\{\tilde{K}_j\}$. Based upon this arrangement, Eq. (49) can be written as

$$\begin{aligned}
\phi_{\text{TPG}} &= \sum_j\sum_{K\in\{\tilde{K}_j\}}\text{Arg}\big[\det\big(F^{(N)}_K\big)\big]\\
&= \sum_j\text{Arg}\big[\det\big(\mathcal{W}^{(N)}_{K_j\to K_j-2p\pi}\big)\big]\\
&= \sum_j\phi_{\text{c.m.}}(K_j).
\end{aligned} \tag{51}$$

In this manner, we have proven that the TBC Berry phase is related to the Berry phase defined through the c.m. momentum state [Eq. (47)].

To better illustrate the relation in Eq. (51), let us consider a fictitious $\nu = 1/2$ system in one dimension. Two specific cases are assumed: there appear (i) twofold-degenerate ground states [Fig. 3(a)] and (ii) fourfold-degenerate ground states [Fig. 3(b)]. For twofold-degenerate ground states, all these c.m. momentum states are connected by the twist angle. The TBC Berry phase only consists of one single multiparticle Wilson loop. For fourfold-degenerate ground states, the ground states can be classified into two sets, and the c.m. momentum states in each set are connected by the twist angle. These c.m. momentum states will form two multiparticle Wilson loops, respectively, and the TBC Berry phase is contributed from these two parts according to Eq. (51).

D. Discussions for few-body systems and many-body systems

For a few-body system in the thermodynamic limit, Eq. (47) can be equivalently written as

$$\phi_{\text{c.m.}} = i\int_0^{2p\pi} dK\ \text{Tr}(A_K). \tag{52}$$

It can be seen that the N-particle Wilson loop in Eq. (47) covers p Brillouin zones. Thus, it is p times the result in Eq. (45), and these two methods are equivalent up to a constant factor. According to Eq. (14), different choices of position definition lead to different relations of unitary transformation for the c.m. momentum state. Similar to the derivation in Sec. III A 3, it can be proved that the change of position definition only leads to an extra constant term. On the other hand, it is proved that this c.m. momentum Berry phase is related to the c.m. position of the multiparticle Wannier state [30,31]. This is also very similar to the single-particle case. In particular, the few-body bound state can be considered an effective single particle [28–37]. The relative distribution is treated as the internal degree of freedom of the effective single particle. It can also be seen that, for few-body systems, the integral with respect to the twist angle is equivalent to the integral with respect to the c.m. momentum when calculating the Berry phase.

For a many-body system, the N-particle Wilson loop only consists of finite eigenstates in the thermodynamic limit, as discussed above. According to Eq. (19), we can find that the c.m. momentum states are connected by the twist angle. The perturbative analysis in Sec. III A 4 implies that, in the many-body case, all these c.m. momentum states only differ by a phase up to the first order of $1/L$ as long as they are connected by the twist angle. Hence, we do not have to calculate the full Wilson loop in this condition. It is sufficient to only calculate the overlap between the starting point K_j and the ending point $K_j - 2p\pi$:

$$\mathcal{W}^{(N)}_{K_j\to K_j-2p\pi} \approx F^{(qN)}_{K_j}, \tag{53}$$

where $[F^{(qN)}_{K_j}]_{m,n}=\langle u^m_{K_j}|u^n_{K_j-qN\delta K}\rangle=\langle u^m_{K_j}|u^n_{K_j-2p\pi}\rangle$ (recall that $\delta K = 2\pi/L$ and $N/L = p/q$). According to Eq. (14), there is $|u^n_{K_j-2p\pi}\rangle = \mathcal{R}_{-2p\pi}|u^n_{K_j}\rangle$. Hence, we have a rather simple expression:

$$\left[F^{(qN)}_{K_j}\right]_{m,n} = \left\langle u^m_{K_j}\middle|\mathcal{R}_{-2p\pi}\middle|u^n_{K_j}\right\rangle. \tag{54}$$

This result means that we only need to compute one of the target states to obtain the Berry phase, which is more efficient when the target states are multifold degenerate.

E. Chern number

Having investigated the Berry phase, below we show that the Chern number can be written as the winding of the Berry phase. Let us consider a 1D system with a time-periodic modulation, dubbed the (1+1)D system, since the time-periodic modulation can be viewed as an artificial dimension [5]. In such a system, the modulation adiabatically changes the lattice potential and results in an adiabatic current [23]. After a pumping period, the Hamiltonian returns to its original form. Under the TBC, we consider a set of gapped target states $\tilde{\mathbf{\Psi}}(\theta,\tau) = (|\tilde{\psi}_1(\theta,\tau)\rangle,\ldots,|\tilde{\psi}_{\mathcal{N}}(\theta,\tau)\rangle)$. Thus we have $\tilde{\mathbf{\Psi}}(\theta+2\pi,\tau) = \tilde{\mathbf{\Psi}}(\theta,\tau+T) = \tilde{\mathbf{\Psi}}(\theta,\tau)$. The Chern number can be written as [9]

$$\begin{aligned} C_{(1+1)\text{D}} &= -\frac{1}{2\pi}\int_0^T d\tau\int_0^{2\pi} d\theta\ \text{Tr}[\tilde{\mathcal{F}}(\theta,\tau)],\\ \tilde{\mathcal{F}}(\theta,\tau) &= i\partial_\tau\tilde{\mathcal{A}}_\theta(\theta,\tau) - i\partial_\theta\tilde{\mathcal{A}}_\tau(\theta,\tau)\\ &\quad + [\tilde{\mathcal{A}}_\tau(\theta,\tau),\tilde{\mathcal{A}}_\theta(\theta,\tau)]. \end{aligned} \tag{55}$$

The commutator term in the non-Abelian Berry curvature $\tilde{\mathcal{F}}(\theta,\tau)$ will vanish after the trace operation; therefore, the Chern number reads as

$$\begin{aligned} C_{(1+1)d} &= -\frac{1}{2\pi}\int_0^T d\tau\int_0^{2\pi} d\theta\ i\partial_\tau[\text{Tr}(\tilde{\mathcal{A}}_\theta)]\\ &\quad + \frac{1}{2\pi}\int_0^T d\tau\int_0^{2\pi} d\theta\ i\partial_\theta[\text{Tr}(\tilde{\mathcal{A}}_\tau)], \end{aligned} \tag{56}$$

where we have exchanged the orders of trace and partial derivative operations. Now, if one integrates the twist angle θ first, the second term will vanish,

$$\begin{aligned} \int_0^{2\pi} d\theta\ i\partial_\theta[\text{Tr}(\tilde{\mathcal{A}}_\tau)] &= i\text{Tr}[\tilde{\mathcal{A}}_\tau(2\pi,\tau) - \tilde{\mathcal{A}}_\tau(0,\tau)]\\ &= 0, \end{aligned} \tag{57}$$

since the Berry connection $\tilde{\mathcal{A}}_\tau(\theta,\tau)$ is a single-valued periodic function. Finally, by exchanging the orders of integral and partial derivative, one can find that the Chern number can be written as a winding of the Berry phase,

$$\begin{aligned} C_{(1+1)d} &= -\frac{1}{2\pi}\int_0^T d\tau\int_0^{2\pi} d\theta\ i\partial_\tau[\text{Tr}(\tilde{\mathcal{A}}_\theta)]\\ &= \frac{1}{2\pi}\int_0^T d\tau\ \partial_\tau\left\{-\int_0^{2\pi} d\theta\ i[\text{Tr}(\tilde{\mathcal{A}}_\theta)]\right\}\\ &= \frac{1}{2\pi}\int_0^T d\tau\ \partial_\tau[\phi_{\text{TBC}}(\tau)], \end{aligned} \tag{58}$$

where the minus sign is relevant to the form of the twist angle. As for 2D systems under the TBC, one can consider one of the twist angles as a modulation parameter, which leads to the same result. Equation (58) suggests that the Chern number can be derived from the Berry phase. According to Eq. (32), we know that the Berry phase under periodic gauge and boundary gauge only differ by a classical polarization $\bar{P}$, which vanishes after a pumping cycle:

$$\int_0^T d\tau\ \partial_\tau\bar{P}(\tau) = \bar{P}(T) - \bar{P}(0) = 0. \tag{59}$$

Since we have established the relation between the TBC Berry phase and the c.m. Berry phase in Sec. III C, we can use the c.m. momentum state to equivalently calculate the Chern number.

IV. DEMONSTRATION VIA INTERACTING AUBRY-ANDRÉ-HARPER MODEL

In this section, we employ a simple but typical 1D topological model, the Aubry-André-Harper (AAH) model [60,61],

to demonstrate the above general framework for both many-body and few-body situations. The AAH model consists of spatial modulations on either the tunneling strength or on-site potentials. The noninteracting AAH model can be viewed as a reduction of the 2D Hofstadter model [62,63], and has been realized in various experimental platforms [64–66]. Thouless points out that adiabatic cyclic modulation in the 1D lattice may lead to quantized pumping of particles, provided that the spectral gap is preserved [9,23]. The topological origin of this quantized pumping much resembles the quantum Hall effect. Later, the charge pumping is associated with the modern theory of polarization [24–26]. By changing the modulation phase, one is able to achieve the well-known Thouless pumping [23,67] via the AAH model. Notably, a special case of AAH model, called the Rice-Mele model [68], has been experimentally realized by loading ultracold atoms into a superlattice [69,70], in which the quantized topological pumping is observed. Recently, the interaction effect in such a model has been experimentally studied [71,72]. During the pumping cycle, the Berry phase will change with the modulation parameter, corresponding to the existence of adiabatic current. Therefore, it is desirable to calculate and compare the TBC and c.m. Berry phases in the same system.

Below we only consider the spatial modulation on the tunneling strength, dubbed the off-diagonal AAH model. The Hamiltonian reads as

$$\hat{H}_{\mathrm{AAH}}(\Phi) = -\sum_{j} (t_j(\Phi)\hat{a}^{\dagger}_{j+1}\hat{a}_j + \mathrm{H.c.}), \tag{60}$$

in which $\hat{a}_i$ ($\hat{a}_i^{\dagger}$) are the annihilation (creation) operators of hard-core bosons,and τ is the modulation parameter. The hopping strengths and the on-site energies are modulated respectively according to $t_j(\Phi) = t_0[1 - \lambda\cos(2\pi bj + \Phi)]$, in which ϕ is the modulation phase and b controls the period of the tunneling strength. Moreover, there may appear gapped eigenstates in both many-body and few-body situations if interaction among particles is added, and we can calculate the Berry phases for them. In the following, the modulated tunneling strength is chosen as $\lambda = 0.5t_0$ with $t_0 = 1$, which is essential to open the energy gap. We also set $b = 1/3$ so that the system's period is $1/b = 3$. Within these parameters, we can obtain three energy bands with Chern number $C = \{-1,\ +2,\ -1\}$ in the single-particle case.

A. Many-body AAH model with long-range interaction

First, let us focus on many-body ground states of the noninteracting AAH model. When the interaction is absent, it is known that the ground state is gapped at integer filling $\nu = N/L = 1$ with nonzero t_0, λ for hard-core bosons. Under the PBC, we utilize the method introduced in Sec. II B to construct and diagonalize the c.m. Bloch Hamiltonian using the exact diagonalization method. One can use the numerical method dubbed the seed-state algorithm introduced in Ref. [30] to efficiently achieve it. The low-lying energy spectrum of the noninteracting AAH model under the PBC is shown in Fig. 4(a). It can be seen that there is a unique and gapped ground state with c.m. momentum $K = 0$. This ground state corresponds to an insulating phase where the lowest band in the single-particle AAH model is occupied. Next,

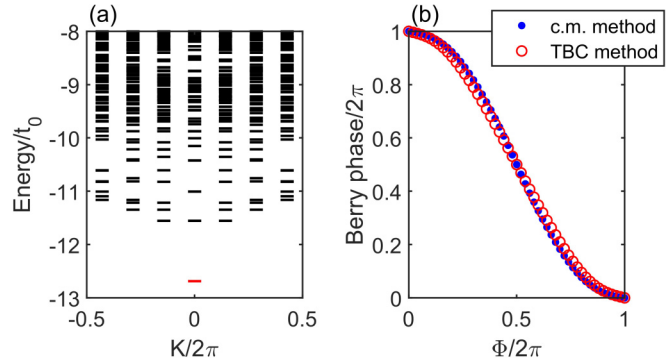

FIG. 4. (a) Low-lying spectrum of the noninteracting off-diagonal AAH model at $\nu = 1$ filling when $\Phi = 0$. The unique gapped ground state is marked by red. (b) Berry phase of the ground state as a function of modulation phase Φ. Red circles are calculated through the TBC [Eq. (24)]. Blue dots are calculated using the c.m. momentum states [Eq. (51)]. We have subtracted the classical polarization for convenience. Parameters are chosen as $N = 7, L = 7$ (the total length of lattice is $L/b = 21$), $V = 0$. Other parameters are fixed as $b = 1/3$, $t_0 = 1$, and $\lambda = 0.5$.

we calculate the Berry phase of this instantaneous ground state via the TBC method [Eq. (24)] and the c.m. momentum method [Eq. (51)]. By applying the c.m. method, according to Eq. (47), the multiparticle Wilson loop for this unique ground state reads as

$$\phi_{\mathrm{c.m.}} = \mathrm{Arg}(\langle u_{K=0}|u_{K=-2\pi}\rangle). \tag{61}$$

Numerical results are shown in Fig. 4(b), in which both methods agree well with each other, despite some tiny differences attributed to the finite-size effect. The Berry phase is a function of the modulation phase and continuously changes from 0 to 2π. According to Eq. (58), the Chern number for this adiabatic pumping process is $C = -1$, indicating a quantized shift of all particles. It can also be confirmed that this result is consistent with the single-particle topological band theory.

To further verify the relation between the two Berry phases, we introduce a long-range interaction among particles,

$$\hat{H}_{\mathrm{Int}}(\Phi) = \hat{H}_{\mathrm{AAH}}(\Phi) + V\sum_{i<j}\frac{\hat{n}_i\hat{n}_j}{|i-j|^3}, \tag{62}$$

which is known to support gapped ground states at fractional filling $\nu \neq 1$ [73–75]. Here, we consider a case of $\nu = 1/2$ filling. The low-lying energy spectrum under the PBC with strong interaction $|t_0/V| \ll 1$ is presented in Fig. 5(a), where two gapped ground states appear at $K = 0$ and $K = \pi$ with near-degenerate energy. Next, we proceed to compute the Berry phases through the c.m. momentum state method and the TBC method numerically [see Fig. 5(b)]. Note that the multiparticle Wilson loop for this twofold ground state reads as

$$\phi_{\mathrm{c.m.}} = \mathrm{Arg}(\langle u_{K=0}|u_{K=-\pi}\rangle\langle u_{K=-\pi}|u_{K=-2\pi}\rangle). \tag{63}$$

It can be seen that the two methods are still in agreement.

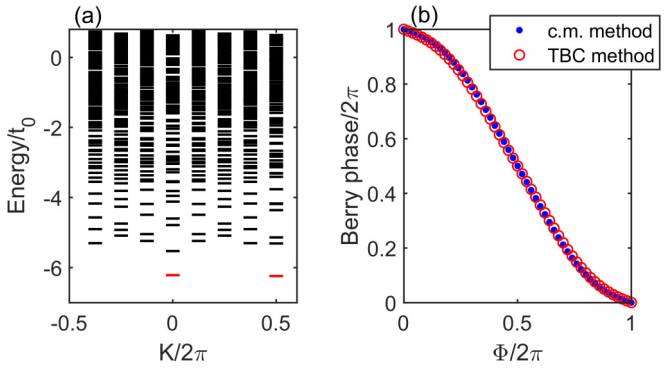

FIG. 5. (a) Low-lying spectrum of the noninteracting off-diagonal AAH model at $\nu = 1/2$ filling when $\Phi = 0$. The two gapped ground states are marked by red. (b) Berry phase of the twofold ground states as a function of modulation phase Φ. Red circles are calculated through the TBC [Eq. (24)]. Blue dots are calculated using the c.m. momentum states [Eq. (51)]. We have subtracted the classical polarization for convenience. Parameters are chosen as $N = 4$, $L = 8$ (the total length of lattice is $L/b = 24$), $V = 50$. Other parameters are fixed as $b = 1/3$, $t_0 = 1$, and $\lambda = 0.5$.

B. Few-body AAH model with nearest-neighbor interaction

Now, let us verify the relation between the TBC Berry phase and the c.m. Berry phase in the few-body system with the total number of particles fixed to $N = 2$. For simplicity, let us consider a nearest-neighbor interaction between particles,

$$\hat{H}_{\rm Int}(\Phi) = \hat{H}_{\rm AAH}(\Phi) + V \sum_j \hat{n}_j \hat{n}_{j+1}. \tag{64}$$

The band structures at $\Phi = 0$ with different interaction strengths are shown in Fig. 6. In the absence of interaction

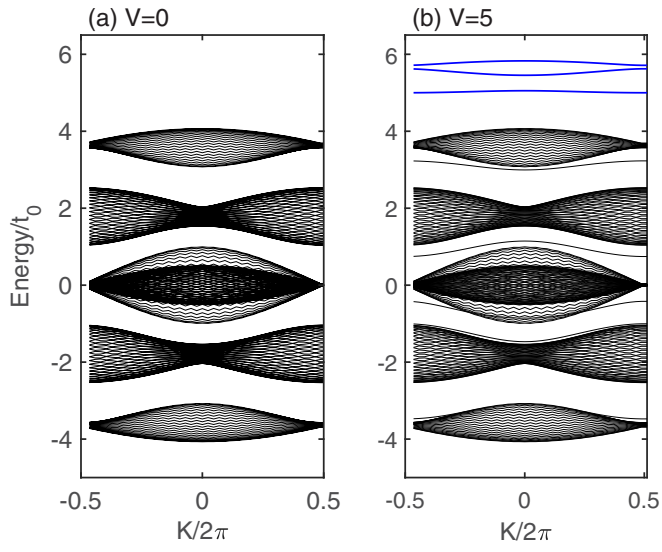

FIG. 6. Instantaneous band structures of the two-particle AAH model at $\Phi = 0$. [(a), (b)] The spectrum under different values of interaction strength $V = 0, 5$. Isolated bands corresponding to strongly bound states are marked by blue in (b). The number of cells is set to $L = 43$ (the total length of lattice is $L/b = 129$), and other parameters are the same as Fig. 4.

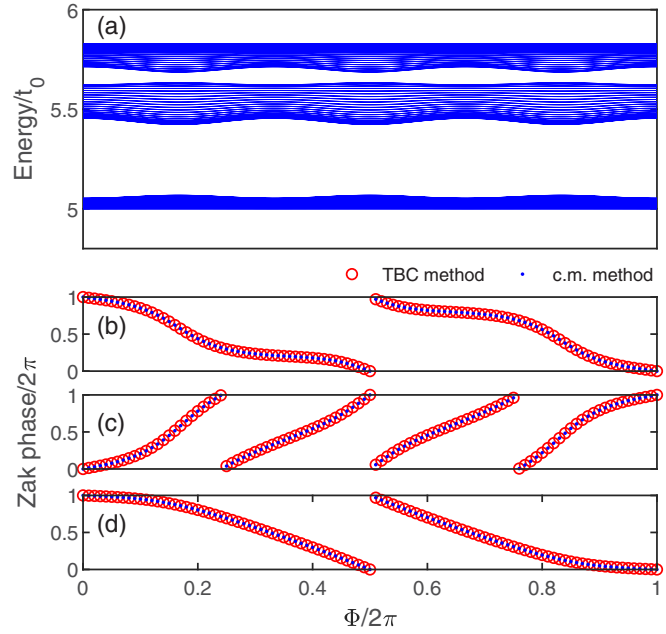

FIG. 7. (a) Energy spectrum of isolated bands in the two-particle AAH model as a function of the modulation phase Φ. [(b)–(d)] Berry phases of the three gapped isolated bands (from top to bottom) as a function of the modulation parameter Φ. Red circles are calculated through the TBC [Eq. (24)]. Blue dots are calculated using the c.m. momentum states [Eq. (51)]. Other parameters are the same as Fig. 6(b).

[Fig. 6(a)], the spectrum is a combination of two single-particle spectra. Because the single-particle system has three gapped bands when $b = 1/3$, there are five continuum bands in the two-particle spectrum. The continuum band corresponds to the nearly independent movement of the two particles. From the top to the bottom, these five continuum bands correspond to five cases: (i) both particles are in the highest (single-particle) band; (ii) either of the particles is in the middle band, while the other one is in the highest band; (iii) both particles are in the middle band; (iv) either of the particles is in the middle band, while the other one is in the lowest band; and (v) both particles are in the lowest band. When the interaction strength is sufficiently strong compared to the band width, isolated bands emerge from continuum bands [see Fig. 6(b)]. These isolated bands correspond to the bound states induced by the particle-particle interaction. Notably, some isolated bands are well separated from the continuum bands, while others are close to the continuum band. The upmost three isolated bands are strongly bound states, and those isolated bands emerging between the continuum bands are weakly bound states.

Next, we investigate the pumping process for the upmost three isolated bands. For simplicity, we fix the interaction strength $V/t_0 = 10$. The spectrum of the three isolated bands presented in Fig. 6(b) is plotted as a function of the modulation phase in Fig. 7(a). It can be seen that the three isolated bands stay gapped during the pumping process. These gapped isolated bands allow us to apply the TBC method [Eq. (24)] and the c.m. momentum method [Eq. (51)] to calculate the instantaneous Berry phases as a function of modulation

phase, respectively [see Figs. 7(b)–7(d). Here, the two-particle Wilson loop reads

$$\mathcal{W}^{(2)}_{K\to K-4\pi} = F^{(2)}_{K} F^{(2)}_{K-2\delta K} \cdots F^{(2)}_{K-4\pi+2\delta K}, \tag{65}$$

where we have chosen that the particle number $N = 2$ and the cell length $L = 43$ are co-prime. Clearly, the TBC approach and the c.m. momentum approach are again in good agreement. According to Eq. (58), the Chern number can be extracted from the winding of the Berry phase. Therefore, from top to bottom in Figs. 7(b)–7(d), we can obtain the Chern number of the three cases, $C = \{-2, +4, -2\}$, which are twice the values of the single-particle bands, respectively.

V. SUMMARY AND DISCUSSIONS

In this article, we have systematically studied the topological invariants defined through the TBC method and the c.m. momentum method in the presence of co-translational symmetry. Under the TBC, one can define a TBC Berry phase through the twist angle. Such a definition is based on the modern polarization theory, where polarization is related to the adiabatic current induced by the change of lattice potential [23–26]. The gauge invariance is discussed in detail, and we provide a useful method to fix the gauge in practical calculations. Notably, we have considered the non-Abelian form of the Berry phase to study the topological property of multiple gapped eigenstates. Hence, it can be applied to noninteracting and interacting systems. Since the twist angle is shown to adiabatically relate different eigenstates, one should involve all these related states to calculate the Berry phase instead of computing them separately.

On the other hand, we have discussed how to construct the c.m. momentum basis according to the co-translation symmetry. To investigate the topological property of the c.m. momentum state, we introduce the multiparticle Wilson loop, which is a generalization of the single-particle version. It allows us to define the c.m. Berry phase, and later it is shown to capture the gauge-invariant geometric phase among gapped multiparticle states. Such a definition makes the c.m. Berry phase applicable for both few-body systems and many-body systems. In addition, this method is also commensurate with the single-particle case.

It is shown that the twist angle connects different c.m. momentum sectors adiabatically. By utilizing the perturbative nature of the twist angle, we uncover the fact that the TBC Berry phase can be equivalently formulated by c.m. momentum states. Importantly, we prove that the TBC Berry phase is deeply related to the c.m. Berry phase obtained from the multiparticle Wilson loop. Since the Chern number can be written as the winding of the Berry phase, the Chern number defined through the TBC can be equivalently computed through the c.m. momentum state. The use of the c.m. momentum state is beneficial for numerical calculations. We can work in the c.m. momentum subspace, which greatly reduces the dimension of the multiparticle Hilbert space. In particular, Eq. (53) suggests a method to efficiently calculate the Berry phase for many-body systems with degenerate ground states.

To verify our arguments, we apply our methods to the AAH model. In the many-body condition, we use the TBC method and the c.m. momentum method to compute the Berry phase of the unique gapped ground state at $\nu = 1$ filling. In the few-body condition, similarly, we investigate the isolated bound-state band induced by interactions through these two methods. In both cases, the c.m. approach is consistent with the conventional TBC method. The numerical results show that the multiparticle Wilson loop can well capture the topological property of the many-body ground state even if there is only one state. This is quite different from the generic single-particle Wilson loop in a noninteracting system or few-body system, in which one needs a number of states to form the loop. With the multiparticle Wilson loop, one can avoid the integration of the twist angle and reduce the computation effort in multiparticle systems.

The equivalence between the topological invariant defined through the TBC and the c.m. momentum state is of importance. It can be seen that the c.m. momentum states of the gapped ground state are correlated, which plays a fundamental role in formulating the topological invariant. This offers a benefit to the understanding of multiparticle topological states. Since the multiparticle Wilson loop formulated by the c.m. momentum states can be applied to both many-body ground states and few-body bands, it is appealing to investigate the relation between the few-body and many-body topological states in future. Meanwhile, the emergence of topological bound states in few-body systems may have some relations to the many-body fractional topological state [76,77]. It is worthwhile to investigate the nature of fractional topological states through the c.m. momentum state method in future.

ACKNOWLEDGMENTS

This work is supported by the National Key Research and Development Program of China (Grant No. 2022YFA1404104), the National Natural Science Foundation of China (Grants No. 12025509 and No. 11874434), and the Key-Area Research and Development Program of GuangDong Province (Grant No. 2019B030330001). L.L. is supported by the NSFC (Grant No. 12247134). Y.K. is partially supported by the NSFC (Grants No. 11904419 and No. 12275365).

APPENDIX A: CO-TRANSLATION SYMMETRY AND CENTER-OF-MASS MOMENTUM FOR FERMIONS

In this section, we demonstrate how to construct the c.m. momentum basis through the co-translation symmetry when the particle is fermionic. In one dimension, we write the N-fermion basis in position space as

$$|x_1, x_2, \ldots, x_N\rangle = \hat{c}^\dagger_{x_1}\hat{c}^\dagger_{x_2}\cdots\hat{c}^\dagger_{x_N}|0\rangle, \tag{A1}$$

in which the position of the particle is in ascending order, $x_1 < x_2 < \cdots < x_N$, and $\hat{c}^\dagger_{x_j}$ is the fermionic creation operator satisfying the anticommutation relation. Under the PBC, there is $\hat{c}^\dagger_{L+1} = \hat{c}^\dagger_1$. When particles are translated across the boundary, we should permute the order of the creation operator to the left-most side. For example, let us consider the co-translation of the following case:

$$\begin{aligned}\hat{T}(\hat{c}^\dagger_1\hat{c}^\dagger_2\cdots\hat{c}^\dagger_L)|0\rangle &= (\hat{c}^\dagger_2\hat{c}^\dagger_3\cdots\hat{c}^\dagger_{L+1})|0\rangle \\ &= (\hat{c}^\dagger_2\hat{c}^\dagger_3\cdots\hat{c}^\dagger_1)|0\rangle.\end{aligned} \tag{A2}$$

To make sure the position of the particle is in ascending order, we have to permute the last creation operator to the left-most side, which yields an overall phase

$$\hat{c}_2^\dagger \hat{c}_3^\dagger \cdots \hat{c}_1^\dagger |0\rangle = e^{i\pi \sum_{j=2}^{L} \hat{n}_j} \hat{c}_1^\dagger \hat{c}_2^\dagger \hat{c}_3^\dagger \cdots |0\rangle. \tag{A3}$$

In other words, for even particle number $N \in 2\mathbb{Z}$ in one dimension, the co-translation operation obeys a twisted boundary condition with $\theta = \pi$, which is also called the *antiperiodic boundary condition*. This can be also derived by performing the Jordan-Wigner transformation to transform the fermionic system to the hard-core bosonic system.

To take into account the quantum statistic effect of fermions in a multiparticle system when constructing the c.m. momentum basis, we should modify Eq. (8) for even particle number. In this case, the antiperiodic boundary condition breaks general co-translation symmetry since $[\hat{H}, \hat{T}] \neq 0$. As demonstrated in Sec. II, it is helpful to transform the twisted boundary condition here from the boundary gauge to the periodic gauge, and then the co-translation symmetry is restored. The fermionic c.m. momentum basis can be thus written as

$$|K, \beta\rangle_{\mathrm{F}} = \frac{1}{\sqrt{C_\beta}} \sum_R e^{iKR} e^{i\frac{\pi}{L}\hat{x}} |R, \beta\rangle. \tag{A4}$$

On the other hand, for odd particle number, the c.m. momentum basis remains the same form as the bosonic one. With this method, our framework on the c.m. momentum state is valid for fermions, and our results on the relation between the TBC and c.m. momentum in Sec. II is still applicable.

In addition, we give a brief discussion for the 2D system. Similarly, one can specify the order of the creation operator in a 1D manner when constructing the position basis in 2D systems. Under the PBC, the co-translation operation for fermions leads to a complicated antiperiodic boundary condition depending on the particle distribution in the lattice. Nevertheless, it is still possible to introduce the periodic gauge to restore the co-translation symmetry, and thus the c.m. momentum basis can be constructed in the same vein.

APPENDIX B: QUASIUNITARITY OF $\mathcal{M}$

Below, we show that the matrix $\mathcal{M}$ mentioned in Eq. (40) is a unitary matrix in the thermodynamic limit. According to Eq. (44), there is

$$\mathcal{M} = \mathbf{\Psi}^\dagger \hat{U}_{2\pi} \mathbf{\Psi}', \quad \mathcal{M}^\dagger = \mathbf{\Psi}'^\dagger \hat{U}_{2\pi}^{-1} \mathbf{\Psi}, \tag{B1}$$

in which $\mathbf{\Psi}' = \mathbf{\Psi}\mathcal{S}$ and $\mathcal{S}$ is an orthogonal matrix that transforms the index μ to μ' according to how the eigenstate flows after the twist angle θ changes for 2π. The vector is normalized: $\mathbf{\Psi}^\dagger\mathbf{\Psi} = \mathbf{\Psi}'^\dagger\mathbf{\Psi}' = I_{\mathcal{N}}$, and $\mathcal{N}$ is the number of target states. Meanwhile, we have $\mathbf{\Psi}\mathbf{\Psi}^\dagger = \mathbf{\Psi}'\mathbf{\Psi}'^\dagger = \sum_\mu |\psi_\mu\rangle\langle\psi_\mu| = 1$ in the subspace spanned by target states. There is

$$\begin{aligned}
\mathcal{M}\mathcal{M}^\dagger &= \mathbf{\Psi}^\dagger \hat{U}_{2\pi} \mathbf{\Psi}' \mathbf{\Psi}'^\dagger \hat{U}_{2\pi}^{-1} \mathbf{\Psi} \\
&= \mathbf{\Psi}^\dagger \hat{U}_{2\pi} \left(\sum_\mu |\psi_\mu\rangle\langle\psi_\mu| \right) \hat{U}_{2\pi}^{-1} \mathbf{\Psi} \\
&= \mathbf{\Psi}^\dagger \left(\sum_\mu |\psi_\mu(2\pi)\rangle\langle\psi_\mu(2\pi)| \right) \mathbf{\Psi},
\end{aligned} \tag{B2}$$

where $|\psi_\mu(\varphi)\rangle$ is the eigenstate under periodic gauge, as already mentioned in the main text. Using the expansion (34) for these states, we find

$$\begin{aligned}
\sum_\mu |\psi_\mu(2\pi)\rangle\langle\psi_\mu(2\pi)| &= \sum_\mu |\psi_\mu\rangle\langle\psi_\mu| + O\left(\frac{1}{L}\right) \\
&= 1 + O\left(\frac{1}{L}\right),
\end{aligned} \tag{B3}$$

which implies that $\sum_\mu |\psi_\mu(2\pi)\rangle\langle\psi_\mu(2\pi)|$ is close to the identity matrix in this subspace. Hence, we find $\mathcal{M}\mathcal{M}^\dagger = I_{\mathcal{N}}$ in the thermodynamic limit. One can also prove that $\mathcal{M}^\dagger\mathcal{M} = I_{\mathcal{N}}$ using the same analysis. In summary, we have shown that the matrix $\mathcal{M}$ is approximately a unitary matrix in the thermodynamic limit. Similar conclusions can be found in Refs. [78,79].

[1] K. v. Klitzing, G. Dorda, and M. Pepper, New Method for High-Accuracy Determination of the Fine-Structure Constant Based on Quantized Hall Resistance, Phys. Rev. Lett. **45**, 494 (1980).

[2] M. Z. Hasan and C. L. Kane, Colloquium: Topological insulators, Rev. Mod. Phys. **82**, 3045 (2010).

[3] X.-L. Qi and S.-C. Zhang, Topological insulators and superconductors, Rev. Mod. Phys. **83**, 1057 (2011).

[4] C. L. Kane, Topological band theory and the $\mathbb{Z}_2$ invariant, in *Contemporary Concepts of Condensed Matter Science* (Elsevier, Amsterdam, 2013), Vol. 6, pp. 3–34.

[5] C.-K. Chiu, J. C. Y. Teo, A. P. Schnyder, and S. Ryu, Classification of topological quantum matter with symmetries, Rev. Mod. Phys. **88**, 035005 (2016).

[6] D. C. Tsui, H. L. Stormer, and A. C. Gossard, Two-Dimensional Magnetotransport in the Extreme Quantum Limit, Phys. Rev. Lett. **48**, 1559 (1982).

[7] R. B. Laughlin, Anomalous Quantum Hall Effect: An Incompressible Quantum Fluid with Fractionally Charged Excitations, Phys. Rev. Lett. **50**, 1395 (1983).

[8] H. L. Stormer, Nobel lecture: The fractional quantum Hall effect, Rev. Mod. Phys. **71**, 875 (1999).

[9] Q. Niu and D. Thouless, Quantised adiabatic charge transport in the presence of substrate disorder and many-body interaction, J. Phys. A: Math. Gen. **17**, 2453 (1984).

[10] Q. Niu, D. J. Thouless, and Y.-S. Wu, Quantized Hall conductance as a topological invariant, Phys. Rev. B **31**, 3372 (1985).

[11] D. Xiao, M.-C. Chang, and Q. Niu, Berry phase effects on electronic properties, Rev. Mod. Phys. **82**, 1959 (2010).

[12] K. Kudo, H. Watanabe, T. Kariyado, and Y. Hatsugai, Many-Body Chern Number without Integration, Phys. Rev. Lett. **122**, 146601 (2019).

[13] R. Resta, Quantum-Mechanical Position Operator in Extended Systems, Phys. Rev. Lett. **80**, 1800 (1998).

[14] H. Watanabe and M. Oshikawa, Inequivalent Berry Phases for the Bulk Polarization, Phys. Rev. X **8**, 021065 (2018).

[15] L. Lin, Y. Ke, and C. Lee, Real-space representation of the winding number for a one-dimensional chiral-symmetric topological insulator, Phys. Rev. B **103**, 224208 (2021).

[16] S.-L. Zhu, Z.-D. Wang, Y.-H. Chan, and L.-M. Duan, Topological Bose-Mott Insulators in a One-Dimensional Optical Superlattice, Phys. Rev. Lett. **110**, 075303 (2013).

[17] Y. Kuno, Disorder-induced Chern insulator in the Harper-Hofstadter-Hatsugai model, Phys. Rev. B **100**, 054108 (2019).

[18] Y. Kuno and Y. Hatsugai, Interaction-induced topological charge pump, Phys. Rev. Res. **2**, 042024(R) (2020).

[19] R. B. Laughlin, Quantized Hall conductivity in two dimensions, Phys. Rev. B **23**, 5632 (1981).

[20] M. Oshikawa and T. Senthil, Fractionalization, Topological Order, and Quasiparticle Statistics, Phys. Rev. Lett. **96**, 060601 (2006).

[21] Y. Huo and R. N. Bhatt, Current Carrying States in the Lowest Landau Level, Phys. Rev. Lett. **68**, 1375 (1992).

[22] L. Rossi and F. Dolcini, Nonlinear current and dynamical quantum phase transitions in the flux-quenched Su-Schrieffer-Heeger model, Phys. Rev. B **106**, 045410 (2022).

[23] D. J. Thouless, Quantization of particle transport, Phys. Rev. B **27**, 6083 (1983).

[24] R. D. King-Smith and D. Vanderbilt, Theory of polarization of crystalline solids, Phys. Rev. B **47**, 1651 (1993).

[25] D. Vanderbilt and R. D. King-Smith, Electric polarization as a bulk quantity and its relation to surface charge, Phys. Rev. B **48**, 4442 (1993).

[26] R. Resta, Macroscopic polarization in crystalline dielectrics: The geometric phase approach, Rev. Mod. Phys. **66**, 899 (1994).

[27] D. J. Thouless, M. Kohmoto, M. P. Nightingale, and M. den Nijs, Quantized Hall Conductance in a Two-Dimensional Periodic Potential, Phys. Rev. Lett. **49**, 405 (1982).

[28] X. Qin, F. Mei, Y. Ke, L. Zhang, and C. Lee, Topological magnon bound states in periodically modulated Heisenberg XXZ chains, Phys. Rev. B **96**, 195134 (2017).

[29] X. Qin, F. Mei, Y. Ke, L. Zhang, and C. Lee, Topological invariant and cotranslational symmetry in strongly interacting multi-magnon systems, New J. Phys. **20**, 013003 (2018).

[30] Y. Ke, X. Qin, Y. S. Kivshar, and C. Lee, Multiparticle Wannier states and Thouless pumping of interacting bosons, Phys. Rev. A **95**, 063630 (2017).

[31] L. Lin, Y. Ke, and C. Lee, Interaction-induced topological bound states and Thouless pumping in a one-dimensional optical lattice, Phys. Rev. A **101**, 023620 (2020).

[32] G. Salerno, M. Di Liberto, C. Menotti, and I. Carusotto, Topological two-body bound states in the interacting Haldane model, Phys. Rev. A **97**, 013637 (2018).

[33] A. M. Marques and R. G. Dias, Topological bound states in interacting Su-Schrieffer-Heeger rings, J. Phys.: Condens. Matter **30**, 305601 (2018).

[34] G. Salerno, G. Palumbo, N. Goldman, and M. Di Liberto, Interaction-induced lattices for bound states: Designing flat bands, quantized pumps, and higher-order topological insulators for doublons, Phys. Rev. Res. **2**, 013348 (2020).

[35] G. Pelegrí, A. M. Marques, V. Ahufinger, J. Mompart, and R. G. Dias, Interaction-induced topological properties of two bosons in flat-band systems, Phys. Rev. Res. **2**, 033267 (2020).

[36] F. Mei, G. Chen, N. Goldman, L. Xiao, and S. Jia, Topological magnon insulator and quantized pumps from strongly-interacting bosons in optical superlattices, New J. Phys. **21**, 095002 (2019).

[37] M. Malki and G. S. Uhrig, Topological magnetic excitations, Europhys. Lett. **132**, 20003 (2020).

[38] M. A. Gorlach and A. N. Poddubny, Interaction-induced two-photon edge states in an extended Hubbard model realized in a cavity array, Phys. Rev. A **95**, 033831 (2017).

[39] Y. Ke, J. Zhong, A. V. Poshakinskiy, Y. S. Kivshar, A. N. Poddubny, and C. Lee, Radiative topological biphoton states in modulated qubit arrays, Phys. Rev. Res. **2**, 033190 (2020).

[40] M. Oshikawa, Commensurability, Excitation Gap, and Topology in Quantum Many-Particle Systems on a Periodic Lattice, Phys. Rev. Lett. **84**, 1535 (2000).

[41] H. Watanabe, Insensitivity of bulk properties to the twisted boundary condition, Phys. Rev. B **98**, 155137 (2018).

[42] M. Oshikawa, Topological Approach to Luttinger's Theorem and the Fermi Surface of a Kondo Lattice, Phys. Rev. Lett. **84**, 3370 (2000).

[43] M. Yamanaka, M. Oshikawa, and I. Affleck, Nonperturbative Approach to Luttinger's Theorem in One Dimension, Phys. Rev. Lett. **79**, 1110 (1997).

[44] E. Lieb, T. Schultz, and D. Mattis, Two soluble models of an antiferromagnetic chain, Ann. Phys. **16**, 407 (1961).

[45] I. Affleck and E. H. Lieb, A proof of part of Haldane's conjecture on spin chains, in *Condensed Matter Physics and Exactly Soluble Models* (Springer, Berlin, 1986), pp. 235–247.

[46] M. Oshikawa, M. Yamanaka, and I. Affleck, Magnetization Plateaus in Spin Chains: "Haldane Gap" for Half-Integer Spins, Phys. Rev. Lett. **78**, 1984 (1997).

[47] O. M. Aksoy, A. Tiwari, and C. Mudry, Lieb-Schultz-Mattis type theorems for Majorana models with discrete symmetries, Phys. Rev. B **104**, 075146 (2021).

[48] B. Hetényi, dc conductivity as a geometric phase, Phys. Rev. B **87**, 235123 (2013).

[49] S. D. Geraedts, J. Wang, E. H. Rezayi, and F. D. M. Haldane, Berry Phase and Model Wave Function in the Half-Filled Landau Level, Phys. Rev. Lett. **121**, 147202 (2018).

[50] T. Hirano, H. Katsura, and Y. Hatsugai, Topological classification of gapped spin chains: Quantized Berry phase as a local order parameter, Phys. Rev. B **77**, 094431 (2008).

[51] M. P. Zaletel, R. S. Mong, and F. Pollmann, Flux insertion, entanglement, and quantized responses, J. Stat. Mech. (2014) P10007.

[52] J.-W. Rhim, J. Behrends, and J. H. Bardarson, Bulk-boundary correspondence from the intercellular Zak phase, Phys. Rev. B **95**, 035421 (2017).

[53] N. J. Higham, *Functions of Matrices: Theory and Computation* (Society for Indistrial and Applied Mathematics, Philadelphia, 2008).

[54] N. Marzari, A. A. Mostofi, J. R. Yates, I. Souza, and D. Vanderbilt, Maximally localized Wannier functions: Theory and applications, Rev. Mod. Phys. **84**, 1419 (2012).

[55] I. Mondragon-Shem, T. L. Hughes, J. Song, and E. Prodan, Topological Criticality in the Chiral-Symmetric AIII Class at Strong Disorder, Phys. Rev. Lett. **113**, 046802 (2014).

[56] E. J. Meier, F. A. An, A. Dauphin, M. Maffei, P. Massignan, T. L. Hughes, and B. Gadway, Observation of the topological Anderson insulator in disordered atomic wires, Science **362**, 929 (2018).

[57] W. A. Benalcazar, B. A. Bernevig, and T. L. Hughes, Electric multipole moments, topological multipole moment pumping, and chiral hinge states in crystalline insulators, Phys. Rev. B **96**, 245115 (2017).

[58] J. A. Marks, M. Schüler, J. C. Budich, and T. P. Devereaux, Correlation-assisted quantized charge pumping, Phys. Rev. B **103**, 035112 (2021).

[59] Z.-P. Cian, H. Dehghani, A. Elben, B. Vermersch, G. Zhu, M. Barkeshli, P. Zoller, and M. Hafezi, Many-Body Chern Number from Statistical Correlations of Randomized Measurements, Phys. Rev. Lett. **126**, 050501 (2021).

[60] P. G. Harper, Single band motion of conduction electrons in a uniform magnetic field, Proc. Phys. Soc. Sect. A **68**, 874 (1955).

[61] S. Aubry and G. André, Analyticity breaking and Anderson localization in incommensurate lattices, Ann. Israel Phys. Soc **3**, 18 (1980).

[62] Y. E. Kraus and O. Zilberberg, Topological Equivalence between the Fibonacci Quasicrystal and the Harper Model, Phys. Rev. Lett. **109**, 116404 (2012).

[63] S. Ganeshan, K. Sun, and S. Das Sarma, Topological Zero-Energy Modes in Gapless Commensurate Aubry-André-Harper Models, Phys. Rev. Lett. **110**, 180403 (2013).

[64] G. Roati, C. D'Errico, L. Fallani, M. Fattori, C. Fort, M. Zaccanti, G. Modugno, M. Modugno, and M. Inguscio, Anderson localization of a non-interacting Bose–Einstein condensate, Nature (London) **453**, 895 (2008).

[65] Y. E. Kraus, Y. Lahini, Z. Ringel, M. Verbin, and O. Zilberberg, Topological States and Adiabatic Pumping in Quasicrystals, Phys. Rev. Lett. **109**, 106402 (2012).

[66] H. P. Lüschen, S. Scherg, T. Kohlert, M. Schreiber, P. Bordia, X. Li, S. Das Sarma, and I. Bloch, Single-Particle Mobility Edge in a One-Dimensional Quasiperiodic Optical Lattice, Phys. Rev. Lett. **120**, 160404 (2018).

[67] L. Wang, M. Troyer, and X. Dai, Topological Charge Pumping in a One-Dimensional Optical Lattice, Phys. Rev. Lett. **111**, 026802 (2013).

[68] M. J. Rice and E. J. Mele, Elementary Excitations of a Linearly Conjugated Diatomic Polymer, Phys. Rev. Lett. **49**, 1455 (1982).

[69] M. Lohse, C. Schweizer, O. Zilberberg, M. Aidelsburger, and I. Bloch, A Thouless quantum pump with ultracold bosonic atoms in an optical superlattice, Nat. Phys. **12**, 350 (2016).

[70] S. Nakajima, T. Tomita, S. Taie, T. Ichinose, H. Ozawa, L. Wang, M. Troyer, and Y. Takahashi, Topological Thouless pumping of ultracold fermions, Nat. Phys. **12**, 296 (2016).

[71] S. de Léséleuc, V. Lienhard, P. Scholl, D. Barredo, S. Weber, N. Lang, H. P. Büchler, T. Lahaye, and A. Browaeys, Observation of a symmetry-protected topological phase of interacting bosons with Rydberg atoms, Science **365**, 775 (2019).

[72] A.-S. Walter, Z. Zhu, M. Gächter, J. Minguzzi, S. Roschinski, K. Sandholzer, K. Viebahn, and T. Esslinger, Breakdown of quantisation in a Hubbard-Thouless pump, arXiv:2204.06561.

[73] Z. Xu, L. Li, and S. Chen, Fractional Topological States of Dipolar Fermions in One-Dimensional Optical Superlattices, Phys. Rev. Lett. **110**, 215301 (2013).

[74] H. Guo, S.-Q. Shen, and S. Feng, Fractional topological phase in one-dimensional flat bands with nontrivial topology, Phys. Rev. B **86**, 085124 (2012).

[75] J. C. Budich and E. Ardonne, Fractional topological phase in one-dimensional flat bands with nontrivial topology, Phys. Rev. B **88**, 035139 (2013).

[76] A. M. Läuchli, Z. Liu, E. J. Bergholtz, and R. Moessner, Hierarchy of Fractional Chern Insulators and Competing Compressible States, Phys. Rev. Lett. **111**, 126802 (2013).

[77] N. Okuma and T. Mizoguchi, Relationship between two-particle topology and fractional Chern insulator, Phys. Rev. Res. **5**, 013112 (2023).

[78] T. A. Loring and M. B. Hastings, Disordered topological insulators via C^*-algebras, Europhys. Lett. **92**, 67004 (2010).

[79] M. B. Hastings and T. A. Loring, Almost commuting matrices, localized Wannier functions, and the quantum Hall effect, J. Math. Phys. **51**, 015214 (2010).